PCCP

Accepted Manuscript

ROYAL SOCIETY OF CHEMISTRY

rsc.li/pccp

On the parallelism between the mechanisms behind chromatography and drug delivery: the role of interactions with stationary phase

View Article Online
DOI: 10.1039/C7CP00832E

Filippo Rossi [a,*,1], Franca Castiglione [a,1], Matteo Salvalaglio [b], Monica Ferro [a], Marta Moioli [a], Emanuele Mauri [a], Maurizio Masi [a] and Andrea Mele [a,c,*]

a Department of Chemistry, Materials and Chemical Engineering "Giulio Natta", Politecnico di Milano, via Mancinelli 7, 20131 Milan, Italy;

b Department of Chemical Engineering, University College London, Torrington Place, London WC1E 7JE, United Kingdom;

c CNR-ICRM, via Luigi Mancinelli 7, 20131 Milan, Italy

* corresponding author, email: filippo.rossi@polimi.it, Tel: (+39) 02 23993145, fax: (+39) 02 23993180;

* corresponding author, email: andrea.mele@polimi.it, Tel: (+39) 02 23993006, fax: (+39) 02 23993180;

[1] these authors equally contributed to this work

DOI: 10.1039/C7CP00832E

ABSTRACT

A huge number of studies and works in drug delivery literature are focused on understanding and modeling transport phenomena, the pivotal point for a good device design. The rationalization of all phenomena involved is fundamental, but several concerns arise leaving many issues unsolved. In order to change point of view we decided to focus our attention on parallelisms between two fields that seem to be very far each other: chromatography and drug release. Taking advantages on the studies conducted by many researchers with chromatographic columns we decided to explain all the phenomena involved in drug delivery considering sodium ibuprofen molecules (IP) as analytes and hydrogel as stationary phase. In particular we considered not only diffusion, but also drug-polymer interactions as adsorption on the stationary phase and drug-drug interactions as analytes aggregation. Hydrogel investigated is a promising formulation made of agarose and carbomer 974p (AC) loaded with IP, a non-steroidal common anti-inflammatory drugs. The self-diffusion coefficient of IP in AC formulations was measured by using an innovative method based on Magic Angle Spinning NMR spectroscopic technique to produce High Resolution (liquid-like) spectra. This method (HR-MAS NMR) is used in combination with pulsed field gradient spin echo (PGSE) liquid-state techniques. The model predictions satisfactorily match with experimental data obtained in water and the gel environment, indicating that the model presented here, despite its simplicity, is able to describe the key phenomena governing the device behavior and could be used to rationalize the experimental activity.

Keywords: chromatography, hydrogel, diffusion, drug delivery, HR-MAS NMR spectroscopy.

INTRODUCTION

Hydrogels are compounds based on cross-linked polymeric materials that due to their hydrophilic nature can absorb large quantity of water, maintaining a distinct three-dimensional structure [1, 2]. In this direction, hydrogels are designed in order to obtain mechanical properties suitable to different application in many fields like drug delivery and tissue engineering [3-5]. Due to their remarkable characteristics like tunable physical, chemical, and biological properties, high biocompatibility and versatility in fabrication hydrogels have emerged as promising materials in the biomedical field [6-8]. Significant progress has been made in the synthesis and fabrication of hydrogels from both natural and synthetic sources for various applications; these include regenerative medicine, drug/gene delivery, stem cell and cancer research, and cell therapy [9, 10]. All these applications consider and use the ability of these three-dimensional polymeric systems to regulate and control the transport of solutes through their three-dimensional network [11-13]. Indeed, effective solute transport is one of the most critical design parameters [14-18]. Mass transport parameters determine how nutrients, gasses, waste products, and bioactive agents, such as growth factors and drugs are exchanged within gels or are delivered by them. Except in hydrogels with very large micropores or forced flow conditions, convection usually does not play a significant role in the movement of solutes through hydrogel matrices and diffusion alone is commonly regarded as the driving transport phenomenon [19, 20]. Despite the high simplicity, in terms of mass transport for chemical engineering applications, several problems rise: available studies often show low or even no accordance with descriptive theories and, more generally, this topic is still much debated [21, 22]. This is mainly due to the fact that theoretical studies on drug delivery systems are centered on pure-Fickian diffusion with degradation and swelling of polymers, not considering any other contribution [23, 24]. In order to put order in this matter we decided to change the common point of view and consider the large amount of theories and models already developed for hydrogels used in chromatography [17, 25, 26].

DOI: 10.1039/C7CP00832E

The use of hydrogels in chromatography is indeed well established both in preparative and analytic techniques [27-29]. These two systems (hydrogels loaded of drugs on one side and with analytes on the other) present several points in common: (*i*) hydrogel matrices work as stationary phase, (*ii*) loaded solute molecules diffuse within the matrix and can interact adsorbing on it (solute-polymer interaction) [30-32]. The main difference resides in the fact that in drug delivery there is no presence of flow rate and so superficial velocity. Following this strategy we considered the classic chromatographic mass balance in order to investigate the role of drug-polymer interactions and diffusion within an hydrogel delivery system. *In silico* results were then compared with the ones collected experimentally in water and in hydrogel environments. The drug investigated in this work is sodium ibuprofene (IP), a member of non-steroidal anti-inflammatory drugs, commonly used for relief from arthritis, fever and as a generic pain reliever [33-35]. The chosen hydrogel, specifically developed for central nervous system repair strategies, was obtained by synthesis from statistical block polycondensation between agarose and carbomer 974P (briefly termed as AC, acronymic of their main components), together with cross-linkers [36, 37]. IP self-diffusion coefficients were measured in water and in gel by means of pulsed magnetic field gradients spin-echo (PGSE) nuclear magnetic resonance (NMR) spectroscopy using the high resolution magic angle spinning (HR-MAS) technique [38-40]. In addition we considered here also the aggregation contribution (drug-drug interaction) that takes place in water and in hydrogel and it is very common in several commonly-used drugs [41, 42]. This approach can represent the joint point between two fields that seem to be very far one from the other: chromatography and drug delivery. The interaction between these two fields may pave the way to a better device design with the possibility to predict and tune different release rates in order to address different medical needs.

EXPERIMENTAL PART

Materials

Carbomer 974P (CAS 151687-96-6) with high molecular weight (about 1 MDa), was purchased by Fagron (The Netherlands), triethylamine (TEA, CAS 121-44-8) with high purity by Sigma-Aldrich (Germany). The solvent used was Phosphate Buffer Saline solution (PBS), purchased by Sigma-Aldrich (Germany). For NMR and HR-MAS analysis deuterated PBS was used to avoid overlapping of ^{1}H signal of IP with those of PBS. The other polymer involved in the reaction is agarose (CAS 9012-36-6), by Invitrogen (USA) with molecular weight of about 300 kDa. Finally, sodium ibuprofen (IP, CAS 31121-93-4) was provided by Sigma-Aldrich (Germany). All materials were used as received.

Molecular modeling of the IP dimerization in water

The dimerization of IP molecules was investigated using well-tempered metadynamics (WTmetaD) simulations [43] with the aim of evaluating the thermodynamic stability of IP dimers in aqueous solution. Three simulations were carried out involving respectively dimers formed by two protonated IP molecules (S1), two deprotonated IP molecules (S2) and both a protonated and a deprotonated IP molecule (S3).

In all cases the IP dimers were embedded in cubic simulation boxes 4.0 nm filled with an appropriate number of water molecules and Na^{+} ions to neutralize the net charge of IP deprotonated molecules. Initial configurations were relaxed with an steepest-descent energy minimization followed by a short NPT equilibration. Both during the equilibration and the production WTmetaD simulations pressure was controlled with the isotropic Parrinello-Rahman barostat [44], while temperature was controlled with the Bussi-Donadio-Parrinello thermostat [45].

The generalized amber force field was used to model IP, with atomic charges determined according to the bcc-AM1 approach [46, 47].

View Article Online
DOI: 10.1039/C7CP00832E

Water was explicitly represented using the TIP3P model. Long-rage electrostatics were included through particle-mesh Ewald approach. Covalent bonds involving hydrogen were restrained with the LINCS algorithm [48] to allow a time step of 2 fs.

WTmetaD simulations were carried out using two collective variables: the distance between centers-of-mass between two IP molecules and the distance between the carbon atoms of the carboxylic acid groups. Repulsive Gaussians were added every 500 steps with an initial height of 1.0 kJ/mol, and a bias-factor of 10. All WTmetaD simulations were carried out with Gromacs 5.0 [49, 50] equipped with PLUMED 2 [51].

Hydrogel synthesis and drug loading

Hydrogel synthesis and drug loading procedure was performed in accordance with previous works [37, 52]. Briefly, Carbomer 974P (0.5 g) was stirred and neutralized to pH 7.4 in deuterated PBS solution. Agarose powder (0.5% w/v) was then added and the system was electromagnetically heated up to 80 °C to induce the beginning of the condensation reactions. Then, IP was added to the polymeric formulation as deuterated aqueous solution, before sol/gel transition. IP was loaded in a concentration range from 5 to 120 mg/mL, in order to clearly explore concentration effects on transport properties. The gelling solution was then placed in steel cylinders (0.5 mL each and with the same dimensions of a standard well in a 48-plate) and left to stabilize at 37 °C until reaching complete gelation. The formation of ester bonds between hydroxyl groups of agarose and carboxyl ones of carbomer was described in previous works, where we discussed the chemical nature of agarose-carbomer based hydrogels [53, 54]. Acronyms of hydrogels are harmonized with previous studies [52]. The three-dimensional structure of a gel network could be described as polymer chains interconnected forming a distribution of mesh sizes filled with water. Mesh size ζ describes the average distance between cross-links in polymer network and could be estimated with Flory-Rehner theory [55, 56].

View Article Online
DOI: 10.1039/C7CP00832E

The complete and exhaustive treatment of Flory-Rehner theory applied to AC hydrogels was studied and presented in previous work [52]: ζ 45 nm, M_C 2500 g/mol, ν_e 28 kmol/cm^3 and porosity ε equal to 0.9.

HR-MAS NMR spectroscopy

The ^{1}H NMR spectra of hydrogel systems were recorded on a Bruker Avance spectrometer operating at 500 MHz proton frequency, equipped with a dual ^{1}H/^{13}C HR-MAS (High Resolution Magic Angle Spinning) probe head for semi-solid samples as presented in previous work [30]. Brielfy hydrogel samples were transferred in a 4 mm ZrO_2 rotor containing a volume of about 12 μL. All the ^{1}H spectra were acquired with a spinning rate of 4 kHz to eliminate the dipolar contribution. Self-diffusion coefficients were measured by Diffusion Ordered correlation Spectroscopy (DOSY) experiments, based on pulsed field gradient spin-echo (PGSE) approach. A pulsed gradient unit capable of producing magnetic field pulse gradients in the *z*-direction up to 53 G·cm^{-1} was used. These experiments were performed using the bipolar pulse longitudinal eddy current delay (BPPLED) pulse sequence. The duration of the magnetic field pulse gradients (δ) and the diffusion times (Δ) were optimized for each sample in order to obtain complete dephasing of the signals with the maximum gradient strength. In each DOSY experiment, a series of 64 spectra with 32k points were collected. For each experiment 32 scans were acquired. For the investigated samples, Δ was set to 0.1 s, while the δ values were in the range 0.7-2 ms. The temperature was set and controlled at 37 °C with an air flow of 535 l·h^{-1} in order to avoid any temperature fluctuations due to sample heating during the magnetic field pulse gradients.

DOI: 10.1039/C7CP00832E

Adsorption kinetics

IP adsorption isotherm in AC gel was determined following literature methods [25]. Small hydrogel samples were suspended in excess of IP solution with different concentrations and stirred for 8 h at 37°C. Then IP concentration (q) present within gels was measured by UV spectroscopy at λ=222 nm [57].

Mathematical Model

The model discussed later on was developed with MatLab© suite, using the *lsqcurvefit* function to match experimental data with the proposed physical chemical description.

Statistical analysis

Where applicable, experimental data were analyzed using Analysis of Variance (ANOVA). Statistical significance was set to p value < 0.05. Results are presented as mean value $\pm$ standard deviation. Spectroscopic data presents a standard deviation of about 5%, due to intrinsic instrumental precision.

RESULTS AND DISCUSSION

Experimental measurement of diffusion coefficients via HR-MAS NMR technique

The measurement of diffusivity could be done experimentally using ^{1}H NMR spectroscopy [58]. This well known technique is very reliable for liquid solutions, on the contrary ^{1}H NMR spectrum of hydrogels is characterized by broad signals due to the residual solid-state effects related to the dipole-dipole coupling. This limitation makes the NMR spectra acquired by conventional liquid state probe heads completely useless for the structural and dynamical characterization of the materials [54] and in this direction the use of HR-MAS allowed us to overcome this limitation [39, 59]. As the matter of fact, HR-MAS NMR spectroscopy is a versatile technique that allows to study heterogeneous suspensions, swellable solids and gels. In the present work, HR-MAS NMR spectroscopy combined with PGSE pulse sequence provides important information on the transport properties of the encapsulated drug (IP) in its environment. This methodology is a powerful method for the direct measurement of self-diffusion coefficient of small molecules confined in a hydrogel matrix. The ^{1}H HR-MAS-NMR spectrum of IP dissolved in AC hydrogel is reported in Figure 1 together with line assignment. The molecular formula of IP and the atom numbering are also shown.

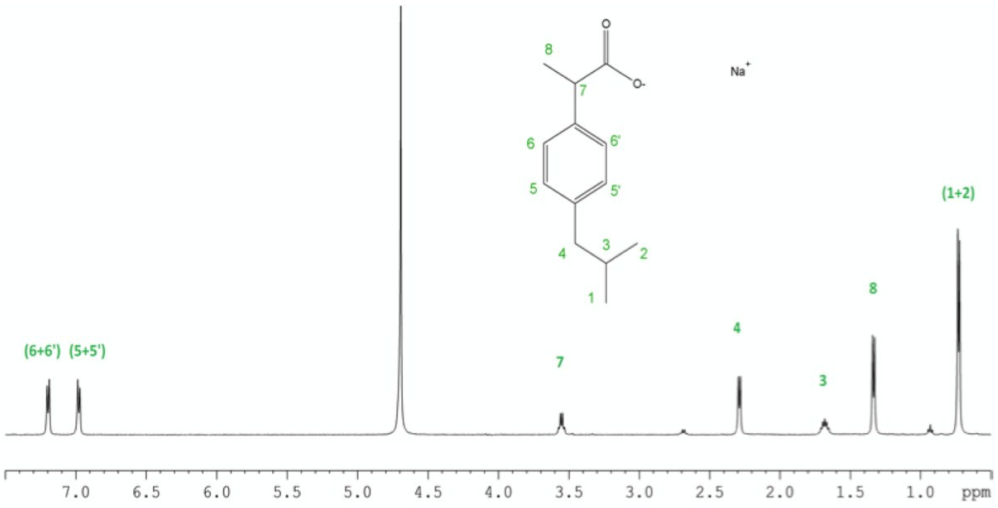

Figure 1. Molecular structure of IP. ^{1}H HR-MAS NMR spectrum of IP loaded within AC hydrogel (75 mg/mL) together with line assignment.

View Article Online
DOI: 10.1039/C7CP00832E

Diffusivity values of IP in AC hydrogels and in water solution are reported in Table 1. As said IP diffusivity was measured both in gel and in water - by HR-MAS NMR and liquid state NMR spectroscopy, respectively - at different concentration to investigate the differences related to the environment of diffusion and concentration influence. It is well visible that diffusion coefficient of IP in D_2O decreases from 6.48 10^{-10} m^2/s to 4.20 10^{-10} m^2/s thus indicating that drug molecules in water interact each other and these interaction become stronger at higher concentration. In gel environment, as observed in water, IP diffusivity decreases as IP concentration increases from 8.12 10^{-10} m^2/s to 4.73 10^{-10} m^2/s. However the most important and counterintuitive result is that, at every IP concentration, diffusity in gel is higher than in water. As said this behavior seems to be unrealistic because, following the Stoke-Einstein equation, diffusivity is inversely proportional to diffusant viscosity. It is indeed well known that, in colloids, diffusivity is the ratio between thermal forces typical of Brownian motion and viscous forces applied by the system (here water solution and gel) to the diffusing agent (here IP). In this case water viscosity is lower compared to the gel and the logic consequence should bring to higher diffusivity values in water rather than in the gel system. In order to justify this mismatch it is obvious that other mechanisms should be considered and taken into account; in this direction we investigated the IP behavior in water environment using MD simulations.

Table 1. Diffusion coefficients of IP at different concentrations in: water solution (D_{water}), in AC hydrogel (D_{gel}) and their ratio respect to IP diffusivity at infinite dilution (D_{gel}/D_{inf} and D_{water}/D_{inf}).

IP concentration [mg/mL]	D_{gel}[a] [m^2/s]	D_{water}[a] [m^2/s]	D_{gel}/D_{inf} [-]	D_{water}/D_{inf} [-]
5	8.12	6.48	0.941	0.762
30	6.21	5.64	0.706	0.664
60	4.98	4.93	0.586	0.580
90	4.88	4.40	0.574	0.518
120	4.73	4.20	0.556	0.494

[a] All values have to be multiplied by 10^{-10}

Molecular modeling of the IP dimerization in water

WTmetaD simulations confirm that within an aqueous environment, which naturally tends to compete with IP-IP hydrogen bonding, IP monomers are the most probable configuration. Nevertheless dimer configurations stabilized by apolar interactions are likely to be present in significant amounts. WTmetaD simulations have been carried out considering systems where the simulated dissociated state can be assumed to be at infinite dilution. As summarized in Table 2, even in these conditions the free energy difference between monomer and dimer states is always well within the 2 k_BT and the equilibrium probability of dimer configurations is between 15 and 27%, depending on the protonation state of the IP molecules forming the dimer.

Table 2. Free energy differences and equilibrium probabilities computed for deprotonated, protonated and mixed IP dimers in water. The equilibrium probability of having two ibuprofen molecules complexed in a dimer configuration has been computed as $p_{eq,dimer} = Z^{-1} \int_{\Omega \in dimer} e^{-\frac{G(S)}{kT}} dS$, where G(S) is the free energy surface obtained as a function of the set of collective variables S, Ω is the configurational space sampled, $\Omega \in dimer$ represents the subset of the conformational space in which dimer configurations are sampled, k is the Boltzmann constant, T the temperature, and Z the partition function computed as $Z = \int_{\Omega} e^{-\frac{G(S)}{kT}} dS$. The equilibrium probability associated to two non-interacting ibuprofen molecules has been computed as $p_{eq,mon} = Z^{-1} \int_{\Omega \notin dimer} e^{-\frac{G(S)}{kT}} dS = 1 - p_{eq,dimer}$.

Label	P_{eq} dimer	P_{eq} monomer	$\Delta G_{D \rightarrow M}$ [kJ/mol]
S1	0.267	0.733	-2.50
S2	0.164	0.836	-4.04
S3	0.234	0.766	-2.94

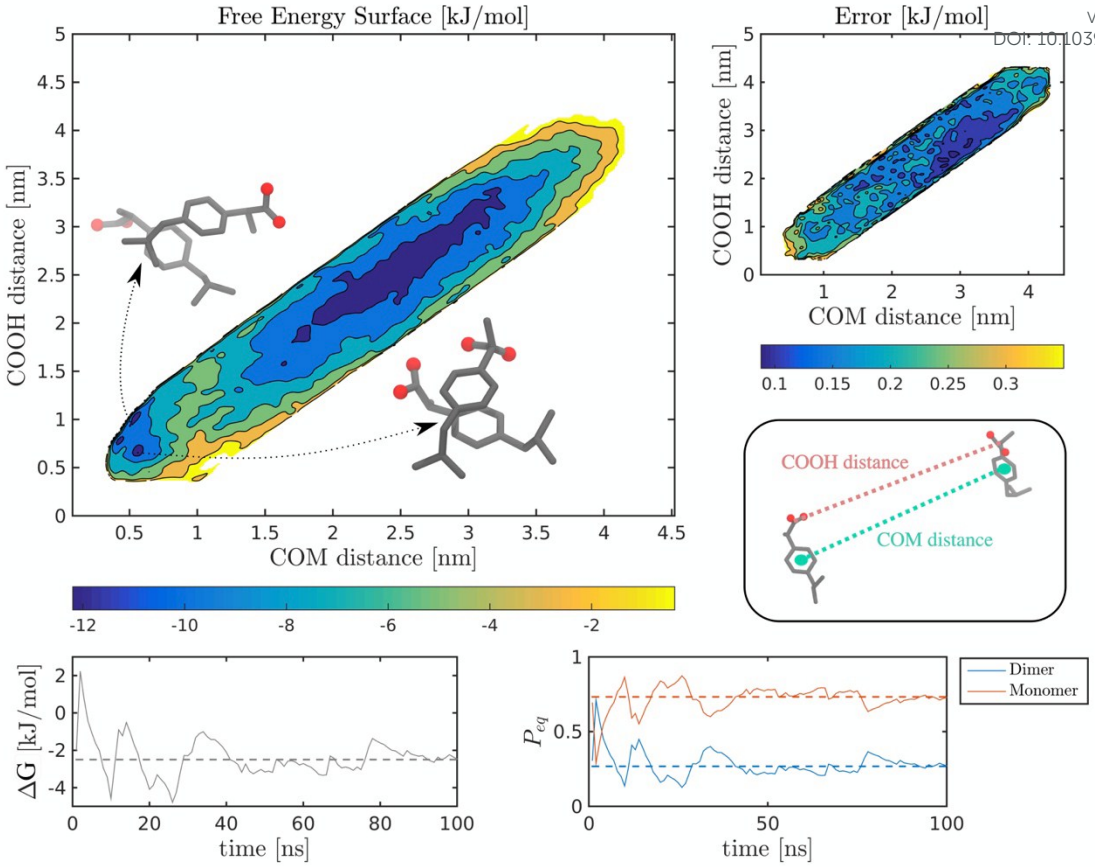

Figure 2. Free energy of dimerization of protonated IP molecules obtained from simulation S1. (*Top left)* Free Energy Surface (FES) as a function of the CVs used to enhance the sampling through WTmetaD. (*Top right)* FES error in the space of CVs evaluated as the standard deviation of the time-independent estimator of the free energy in the CVs space. *(Bottom-left)* Free energy difference between dissociated and dimer-like states as a function of simulation time. *(Bottom-right)* quilibrium probabilities of undissociated and dissociated states. Similar results, obtained for simulations S2 and S3 are reported as supplementary material.

Modeling IP diffusion coefficients in water

As said above the decrease of IP diffusivity as IP concentration increases should be explained before considering the hydrogel environment. A possible explanation of this trend resides in the fact that drug molecules in water solution can aggregate and form oligomers. On the opposite in case studies with drugs that cannot aggregate there is no decrease in drug diffusivity as their concentration increases [30].

View Article Online
DOI: 10.1039/C7CP00832E

Not only from our MD studies but also from literature it is well known that IP revealed a strong tendency to form aggregates such as dimers of either cyclic or linear geometry, which somehow seems to control molecular mobility of that drug [60, 61]. We calculated the equilibrium constants for the dimerization obtained from MD studies (1.6 L/g) and we used in model studies. Molecular simulations presented in previous paragraph suggest that dimer configurations, predominantly stabilized by apolar interactions, account for a significant fraction (20 to 30%) of the configurations at equilibrium. We could calculate diffusivity in water as:

$$D_{water} = \frac{C_M}{C_{tot}} \cdot D_M + \frac{C_D}{C_{tot}} \cdot D_D \quad (1)$$

where C_M is monomer concentration, C_D is dimer concentration and C_{tot} the total IP present, D_M is monomer diffusivity, D_D is dimer diffusivity. In Figure 3 results about mathematical modeling are presented together with experimental data. In particular the two lines are related to two different assumptions: (*a*) only monomer present, $C_{tot} = C_M$ (red); (*b*) monomers and dimers present, $C_{tot} = C_M + 2C_D$ (blue). It is evident that the introduction of the terms related to dimers is fundamental in order to understand the phenomena involved and match the experimental data. In addition IP aggregation increases as IP concentration increases with a consequent reduction in term of diffusivity value.

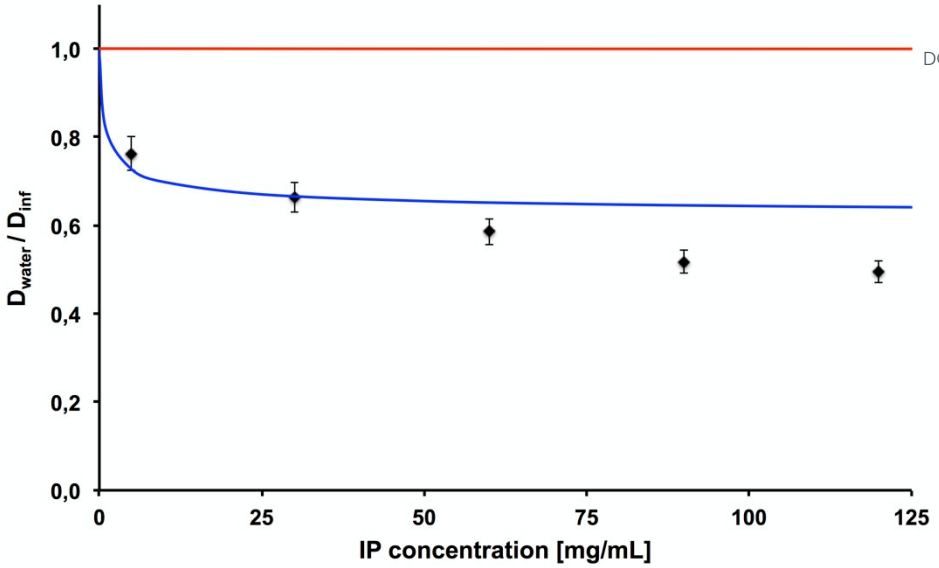

Figure 3. Diffusion normalized coefficients (D_{water}/D_{inf}), experimental data (dots) and model trend (lines): a) red, only monomers; b) blue, monomers and dimers.

Modeling IP diffusion coefficients in gel

As shown in previous works [54], the classic Fick model applied to the drug release experiments provides reliable diffusion coefficient for low concentration of drugs, but cannot be used to study the concentration effect on mass transport. It is well known that, in the absence of drug concentration gradient (as in the present case), drug release rate is not expected to be influenced by its concentration [62]. Drug motion through the three-dimensional network is influenced by the environment and by the other drug molecules. This represents the joint point with chromatography if we consider also in this case polymeric hydrogel network as stationary phase. In particular starting from mass balance used in chromatography we propose here a model able to describe the experimental behavior of drug diffusivity. The model is based on the hypotheses here listed: i) IP molecules can be adsorbed on the three-dimensional polymeric network only if it is in the monomeric state. The mechanism of adsorption of IP on the polymeric network is currently under investigation and no clear-cut conclusion can be metioned at this stage.

View Article Online
DOI: 10.1039/C7CP00832E

However, in analogy to recently reported research on the adsorption of IP in mesomorphous materials, a possible role of hydrogen-bonding between carboxylate group of IP and the hydroxyl groups present in the agarose units could be invoked [63]. Accordingly, the attractive polymer-IP interactions would provide the driving force to overcome the electrostatic repulsion between the negatively charged polymer sites and the ionized carboxylic groups of monomeric IP. The adsorption step reduces thus the contribution of any drug aggregation phenomena. As a consequence, at low values of IP concentration (lower than q^{∞} presented in Figure 5) the most important phenomenon is adsorption within hydrogel pores that reduce the amount of IP available for the formation of dimers; ii) As the IP amount is increased, the adsorption sites are progressively saturated and then IP is capable to diffuse more quickly, in a comparable way with water environment and driven only by the concentration gradient. The rationale for this is based on the observation that the ratio between the mean gel network mesh size and the mean IP hydrodynamic radius that is extremely low: diffusant molecules are mobile inside the entangled hydrogel network. The adsorption mechanism is thus expected to play a dominant role at low IP concentration while it is negligible for higher drug concentration. Previous work by Barbucci and coworkers [34] on *in vivo* application of IP release from hydrogels for the local treatment of chondral lesions in the knee reveals the therapeutic efficacy for concentration equal to 1.5 mg/mL. Redpath and coworkers [35] examined the effects of sodium ibuprofen on the major proinflammatory cytokine tumor necrosis factor and also in this case they considered low value of IP concentration (0.3 mg/mL).

As reported, at low drug concentration, where drug showed high efficacy, the adsorption phenomenon should be considered when describing the drug transport mechanisms. A pictorial representation of the model is shown in Figure 4 where the solid lines represent the AC matrix, the red circles represent the IP molecules adsorbed on the network backbone, the green circles represent IP molecules that are free to move within the network. IP molecules may either undergo adsorption or diffusion.

View Article Online
DOI: 10.1039/C7CP00832E

The latter points are sketched in Figure 4: the green arrows indicate IP monomers diffusion within the polymeric network, while the red arrows show the subsequent adsorption onto the polymer matrix. If all adsorption sites are saturated, IP monomers continue to diffuse, they are likely to collide with other IP monomers (black arrow) and can form dimers.

The experimental diffusion constants detected are the rapid-exchanged values resulting from the weighted average of both the adsorbed and free diffusion rates.

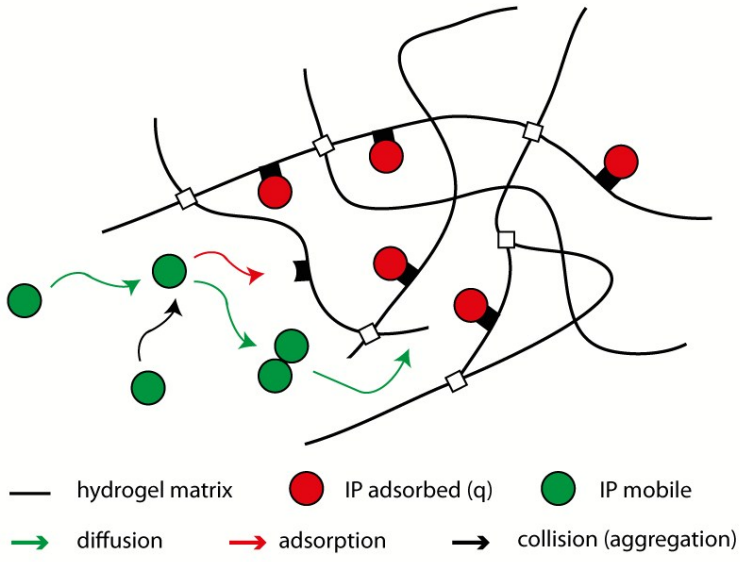

Figure 4. Pictorial representation of the partitioning model.

At this stage, we propose a mathematical model accounting for the steps described above starting from chromatographic studies [32, 64]. The adsorbed IP amount is given by q, as determined from the adsorption Langmuir isotherm (Figure 4) [25]. The isotherm is highly favorable at low drug concentration. Thus a Langmuir isotherm was used to fit the data according to the following equation:

$$q = \frac{q^{\infty} \cdot K \cdot C_G}{1 + K \cdot C_G} \qquad (2)$$

View Article Online
DOI: 10.1039/C7CP00832E

where q^{∞} is the maximum total adsorbed concentration of IP and C_G is the IP concentration within the hydrogel. Fitted line is presented in Figure 5 and calculated parameters are: $q^{\infty} = 34.8$ mg/cm^3 and K = 50 cm^3/mg.

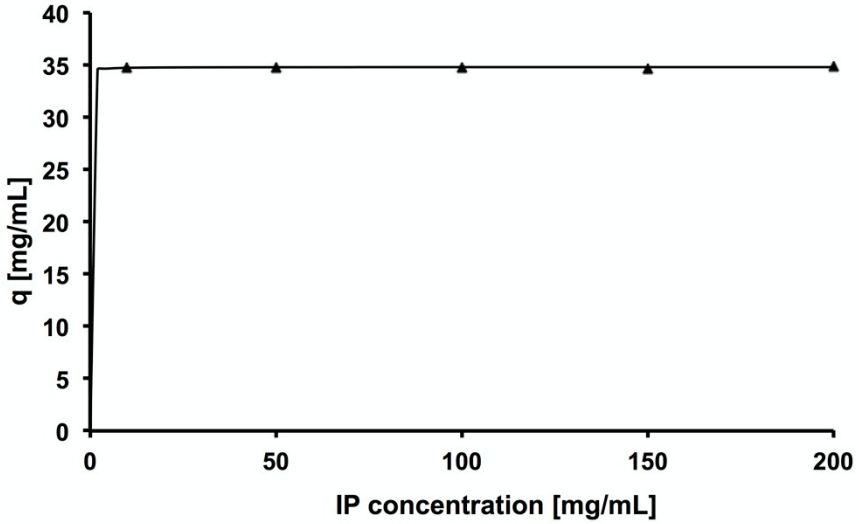

Figure 5. Adsorption isotherm for IP on AC hydrogel. Lines are based on Eq. 2.

The joint contribution of diffusion and adsorption can be described by Eq. 4 considering, as starting point, the mass balance of chromatrographic columns [32, 65]:

$$\varepsilon \cdot D_{water} \cdot \frac{\partial^2 C_G}{\partial x^2} - u \cdot \frac{\partial C_G}{\partial x} = \varepsilon \cdot \frac{\partial C_G}{\partial t} + (1-\varepsilon) \cdot \frac{\partial q}{\partial t} \quad (3)$$

where ε is the gel porosity calculated in previous works [54], C_G is IP concentration within the hydrogel, q is defined in Eq. 2 and *u* is the superficial velocity of chromatographic columns. Generally in chromatography the first term that takes into account diffusion is neglected. Here we consider its contribution and we do not consider the second one because, as said, here there is no presence of pressure that induce a flow rate typical of analytes. The convection term is so equal to zero due to the absence of forced motion within hydrogel polymeric network.

View Article Online
DOI: 10.1039/C7CP00832E

From Eq. 3 we can assume the following assumption:

$$\frac{\partial q}{\partial t} \cong \frac{\partial q}{\partial C_G} \cdot \frac{\partial C_G}{\partial t} \tag{4}$$

so:

$$\frac{\partial q}{\partial C_G} = \frac{q^{\infty} \cdot K}{\Delta^2} \tag{5}$$

where $\Delta = 1 + K \cdot C_G$. We can easily rewrite Eq. 3 as:

$$\varepsilon \cdot \frac{\partial C_G}{\partial t} = \varepsilon \cdot D_{water} \cdot \frac{\partial^2 C_G}{\partial x^2} - (1-\varepsilon) \cdot \frac{\partial C_G}{\partial t} \cdot \frac{q^{\infty} \cdot K}{\Delta^2} \tag{6}$$

Eq. 6 may be rewritten as:

$$\frac{\partial C_G}{\partial t} = \left[\frac{\varepsilon \cdot D_{water}}{\left(\varepsilon + (1-\varepsilon) \cdot \frac{q^{\infty} \cdot K}{\Delta^2}\right)} \right] \cdot \frac{\partial^2 C_G}{\partial x^2} \tag{7}$$

If we consider the second Fick's law [19, 66] the term contained within square bracket is a diffusivity and, in this case, IP diffusivity in gel environment (D_{gel}):

$$D_{gel} = \frac{\varepsilon \cdot D_{water}}{\left(\varepsilon + (1-\varepsilon) \cdot \frac{q^{\infty} \cdot K}{\Delta^2}\right)} \tag{8}$$

considering Eq. 1 D_{gel} can be rewritten as:

$$D_{gel} = \frac{\varepsilon}{\left(\varepsilon + (1-\varepsilon) \cdot \frac{q^{\infty} \cdot K}{\Delta^2}\right)} \cdot \left(\frac{C_M}{C_{tot}} \cdot D_M + \frac{C_D}{C_{tot}} \cdot D_D \right) \tag{9}$$

The model was tested against the experimental values presented in Table 1. The experimental and calculated data are presented in Figure 6.

The good agreement between model (line) and experiments (■) underlines that adsorption isotherm together with diffusion through pores and aggregation can describe the mechanisms involved in IP release from 3D polymeric network. In particular: (1) the drug is first partitioned and adsorbed on pores present in hydrogel three-dimensional matrix.

The amount of adsorbed drug is given by q^{∞} determined from the adsorption isotherm; (2) at higher drug concentration all adsorption sites are saturated and transport occurs by diffusion with a driving force determined by IP concentration gradient.

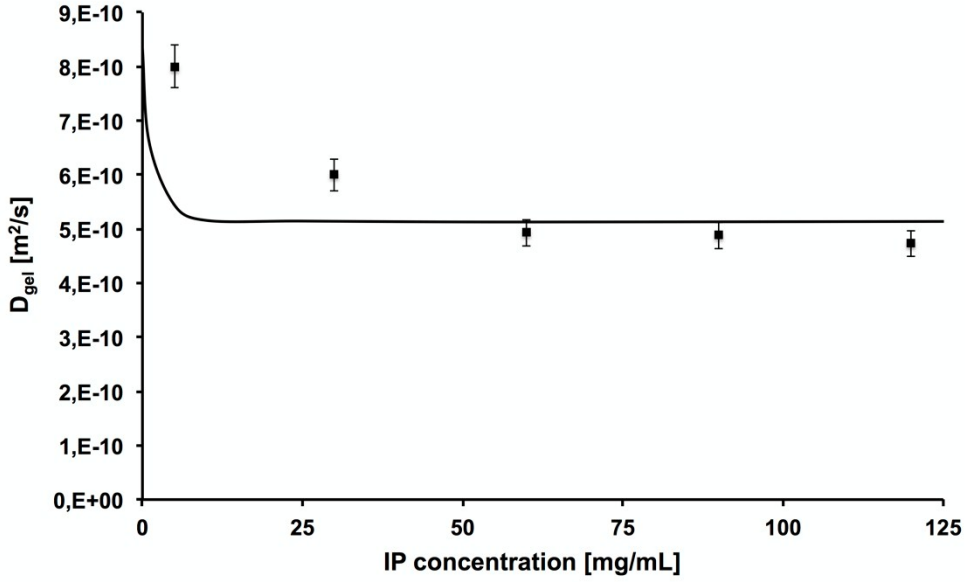

Figure 6. Diffusion coefficients in gel environment, experimental data (dots) and model trend (lines).

Oligomers concentration in water and in gel

The mismatch between Stoke-Einstein equation and diffusivity experimental obtained with HR-MAS technique, could be explained with different amount of oligomers in the gel compared to water solution. In particular, the adsorption mechanism, especially active at low drug concentration, decreases the amount of the available monomers. In Figure 7A the curves related to monomers in water and the gel are presented: the lower amount of monomers at low drug concentration in the gel reveals that the adsorption process depresses the amount of IP capable to diffuse through the system. Moreover, higher IP concentration tends to offset the difference between gel and water because all of the adsorption sites are saturated and the residual solute is free to move and aggregate.

View Article Online
DOI: 10.1039/C7CP00832E

Trends related to dimers in gel (line) and in water (dashed line) are presented in Figure 7B. In accordance with Figure 7A the amount of dimers in gel is lower than in water, underlining the fact that hydrogel systems can prevent their formation.

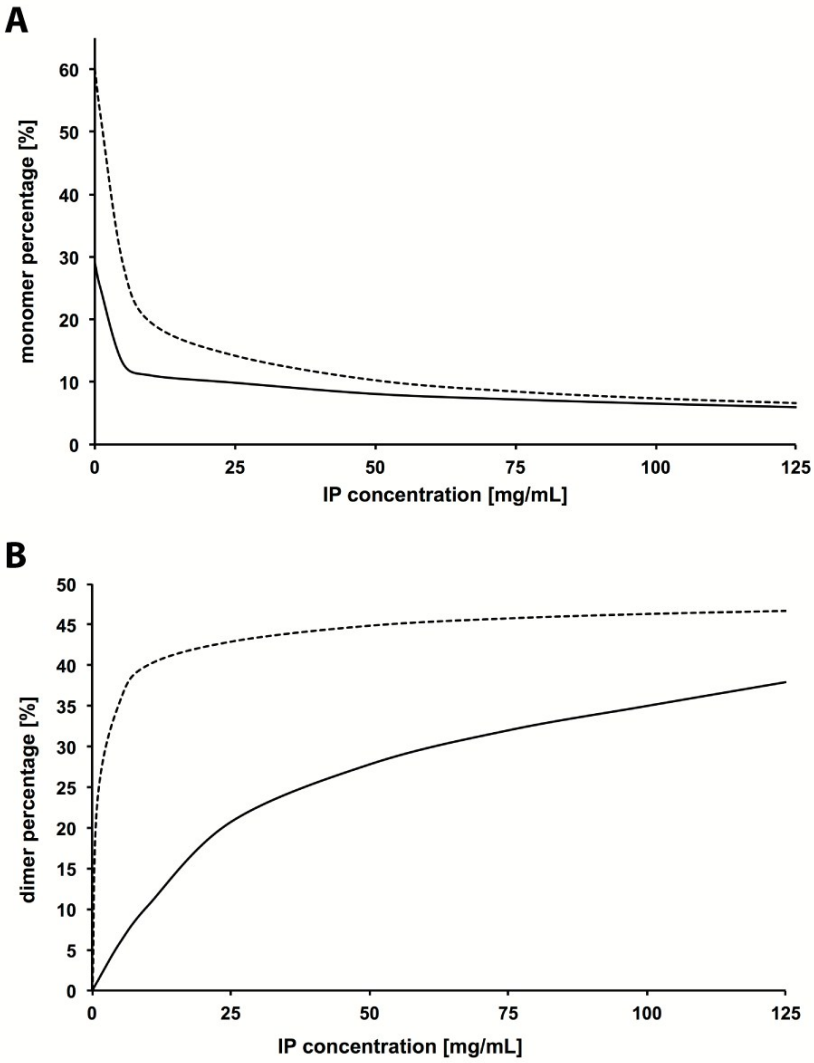

Figure 7. Oligomers percentage in water (dashed line) and in gel (line): (A) monomers; (B) dimers.

Role of porosity

Starting from Figure 7 we investigated other scenarios in order to understand drug-polymer and drug-drug interactions with the aim of controlling and tuning the release rates of IP. The adsorption kinetics becomes slower as gel porosity decreases and consequently the adsorption contribution: for this reasons the amounts of monomers and dimers available decrease as porosity increases.

Tuning hydrogel porosity seems to be a promising method to control mass transport through network pores. In Figure 8 is presented the dependence of diffusivity in gel on hydrogel porosity: decreasing gel porosity it is evident that the adsorption kinetics is slower. In particular, at IP concentrations at which the adsorption mechanism is not negligible, the concentration increases with decreasing porosity.

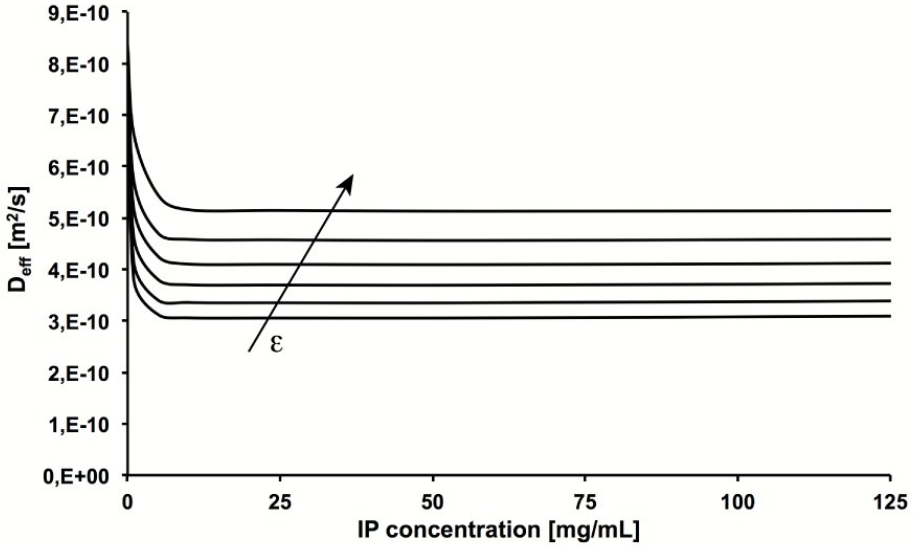

Figure 8. Diffusion coefficients of IP in gel environment tuning hydrogel porosity ε.

CONCLUSIONS

View Article Online
DOI: 10.1039/C7CP00832E

The complete understanding of phenomena involved in drug delivery is pivotal for a good and proper device design. In particular the ability to reduce burst effect and control release rates could guarantee the possibility to solve different medical problems. Mathematical modeling around drug delivery is essentially built around the study of diffusion where only swelling and degradation of polymers are taken into account. Considering the common nature of hydrogels as stationary phase for drugs and analytes, we decided to transfer the knowledge of transport phenomena from chromatography to drug delivery. The purpose of such modeling activity, as mentioned, is to provide a simple but powerful tool to understand the influence of design parameters on drug transport: this also allows a smart device design, tailoring the final product according to the specific needs. In particular solute adsorption is presented as the key mechanism: on one side influence drug motion and on the other reduce the amount of drug able to aggregate in oligomers. This phenomenon is more important at low drug concentration: here adsorption contribution seems to be higher and could not be neglected with a consequent lower amount of monomers present in gel than in water. Increasing drug concentration, when all adsorption sites are saturated, monomers free in the network are subjected to aggregation in dimers. From an applicative point of view, it is thus possible to optimize the experimental activity, which can be expensive and time-consuming. This approach could allow to pass from a classic “trial and error” through a “model driven” experimental modus operandi.

ACKNOWLEDGMENTS

Authors would like to thank Prof. Morbidelli for fruitful discussion.

View Article Online
DOI: 10.1039/C7CP00832E

List of symbols

C_G	IP concentration in gel, mg/mL
C_M	monomer concentration, mg/mL
C_D	dimer concentration, mg/mL
D_{gel}	IP diffusivity in hydrogel, m^2/s
D_{inf}	IP diffusivity at infinite dilution, m^2/s
D_M	monomer diffusivity in water, m^2/s
D_D	dimer diffusivity in water, m^2/s
D_{water}	IP diffusivity in water, m^2/s
K	Langmuir isotherm parameter
K_d	equilibrium constant for IP dimerization
M_C	average molecular weight between two following cross-links, g/mol
P	equilibrium probability
q	adsorbed concentration, mg/cm^3
q^∞	maximum adsorbed concentration, mg/cm^3

Greek symbols

ε	porosity
ζ	hydrogel mean mesh size, nm
ν_e	cross-linking density, mol/cm^3

References

1. N. Annabi, A. Tamayol, J. A. Uquillas, M. Akbari, L. E. Bertassoni, C. Cha, G. Camci-Unal, M. R. Dokmeci, N. A. Peppas and A. Khademhosseini, *Adv. Mater.*, 2014, 26, 85-124.
2. B. V. Slaughter, S. S. Khurshid, O. Z. Fisher, A. Khademhosseini and N. A. Peppas, *Adv. Mater.*, 2009, 21, 3307-3329.
3. F. Rossi and M. van Griensven, *Tissue Eng. A*, 2014, 20, 2043-2051.
4. R. Langer, *Adv. Mater.*, 2009, 21, 3235-3236.
5. S. Ahadian, R. B. Sadeghian, S. Salehi, S. Ostrovidov, H. Bae, M. Ramalingam and A. Khademhosseini, *Bioconjugate Chem.*, 2015, 26, 1984-2001.
6. F. Ullah, M. B. H. Othman, F. Javed, Z. Ahmad and H. M. Akil, *Mat Sci Eng C-Mater*, 2015, 57, 414-433.
7. K. Yue, G. Trujillo-de Santiago, M. M. Alvarez, A. Tamayol, N. Annabi and A. Khademhosseini, *Biomaterials*, 2015, 73, 254-271.
8. R. R. Xue, X. Xin, L. Wang, J. L. Shen, F. R. Ji, W. Z. Li, C. Y. Jia and G. Y. Xu, *Phys. Chem. Chem. Phys.*, 2015, 17, 5431-5440.
9. S. Merino, C. Martin, K. Kostarelos, M. Prato and E. Vazquez, *Acs Nano*, 2015, 9, 4686-4697.
10. S. Park and K. M. Park, *Polymers-Basel*, 2016, 8.
11. E. E. Antoine, P. P. Vlachos and M. N. Rylander, *Tissue Eng Part B-Re*, 2014, 20, 683-696.
12. I. Vladescu, O. Lieleg, S. Jang and K. Ribbeck, *J. Pharm. Sci.*, 2012, 101, 436-442.
13. B. Rossi, V. Venuti, A. Mele, C. Punta, L. Melone, F. D'Amico, A. Gessini, V. Crupi, D. Majolino, F. Trotta and C. Masciovecchio, *Phys. Chem. Chem. Phys.*, 2016, 18, 12252-12259.
14. J. Karger, *Chemphyschem*, 2015, 16, 24-51.
15. J. Siepmann and N. A. Peppas, *Adv. Drug Deliv. Rev.* , 2001, 48, 139-157.
16. J. Siepmann and K. Siepmann, *Int. J. Pharm.*, 2008, 364, 328-343.
17. R. K. Lewus and G. Carta, *Ind. Eng. Chem. Res.*, 2001, 40, 1548-1558.
18. M. Kojic, M. Milosevic, S. H. Wu, E. Blanco, M. Ferrari and A. Ziemys, *Phys. Chem. Chem. Phys.*, 2015, 17, 20630-20635.
19. G. S. Crank, *Diffusion in Polymers*, Academic, New York, 1968.
20. D. Caccavo, S. Cascone, G. Lamberti and A. A. Barba, *Mol. Pharm.*, 2015, 12, 474-483.
21. L. Masaro and X. X. Zhu, *Prog. Polym. Sci.*, 1999, 24, 731-775.
22. I. Kohli and A. Mukhopadhyay, *Macromolecules*, 2012, 45, 6143-6149.
23. N. A. Peppas and B. Narasimhan, *J. Control. Release*, 2014, 190, 75-81.
24. C. C. Lin and A. T. Metters, *Adv. Drug Deliv. Rev.*, 2006, 58, 1379-1408.
25. E. B. Schirmer and G. Carta, *Aiche J.*, 2009, 55, 331-341.
26. P. Saremirad, J. A. Wood, Y. Zhang and A. K. Ray, *J. Chromatogr. A*, 2014, 1370, 147-155.
27. J. Lu, W. F. Zhang, Y. H. Zhang, W. J. Zhao, K. Hu, A. J. Yu, P. Liu, Y. J. Wu and S. S. Zhang, *J. Chromatogr. A*, 2014, 1350, 61-67.
28. W. J. Zhao, W. J. Wang, H. Chang, S. W. Cui, K. Hu, L. J. He, K. Lu, J. X. Liu, Y. J. Wu, J. Qian and S. S. Zhang, *J. Chromatogr. A*, 2012, 1251, 74-81.
29. J. Kobayashi, A. Kikuchi, K. Sakai and T. Okano, *J. Chromatogr. A*, 2002, 958, 109-119.
30. F. Rossi, F. Castiglione, M. Ferro, P. Marchini, E. Mauri, M. Moioli, A. Mele and M. Masi, *Chemphyschem*, 2015, 16, 2818-2825.
31. G. Carta and A. Jungbauer, *Protein Chromatography - Process Development and Scale-up*, Wiley-VCH, 2010.
32. M. D. LeVan and G. Carta, in *Perry's Chemical Engineers' Handbook*, McGraw-Hill, 2007, ch. Section 16.
33. P. Manesiotis, Q. Osmani and P. McLoughlin, *J. Mater. Chem.*, 2012, 22, 11201-11207.
34. R. Barbucci, M. Fini, G. Giavaresi, P. Torricelli, R. Giardino, S. Lamponi and G. Leone, *J Biomed Mater Res B*, 2005, 75B, 42-48.

35. M. Redpath, C. M. G. Marques, C. Dibden, A. Waddon, R. Lalla and S. MacNeil, *Br. J. Dermatol.*, 2009, 161, 25-33.
36. S. Papa, F. Rossi, R. Ferrari, A. Mariani, M. De Paola, I. Caron, F. Fiordaliso, C. Bisighini, E. Sammali, C. Colombo, M. Gobbi, M. Canovi, J. Lucchetti, M. Peviani, M. Morbidelli, G. Forloni, G. Perale, D. Moscatelli and P. Veglianese, *Acs Nano*, 2013, 7, 9881-9895.
37. I. Caron, F. Rossi, S. Papa, R. Aloe, M. Sculco, E. Mauri, A. Sacchetti, E. Erba, N. Panini, V. Parazzi, M. Barilani, G. Forloni, G. Perale, L. Lazzari and P. Veglianese, *Biomaterials*, 2016, 75, 135-147.
38. J. E. Jenkins, M. R. Hibbs and T. M. Alam, *Acs Macro Lett.*, 2012, 1, 910-914.
39. T. M. Alam and M. R. Hibbs, *Macromolecules*, 2014, 47, 1073-1084.
40. G. Perale, F. Rossi, M. Santoro, P. Marchetti, A. Mele, F. Castiglione, E. Raffa and M. Masi, *J. Biomed. Nanotechnol.*, 2011, 7, 476-481.
41. S. Lerdkanchanaporn and D. Dollimore, *J. Therm. Anal. Calorim.*, 1997, 49, 879-886.
42. W. Ali, A. C. Williams and C. F. Rawlinson, *Int. J. Pharm.*, 2010, 391, 162-168.
43. A. Barducci, G. Bussi and M. Parrinello, *Phys Rev Lett*, 2008, 100, 020603.
44. M. Parrinello and A. Rahman, *J Appl Phys*, 1981, 52, 7182-7190.
45. G. Bussi, D. Donadio and M. Parrinello, *J Chem Phys*, 2007, 126.
46. W. Cornell, P. Cieplak, C. Bayly, I. Gould, K. Merz, D. Ferguson, D. Spellmeyer, T. Fox, J. Caldwell and P. J. Kollman, *J Am Chem Soc*, 1995, 117, 5179-5197.
47. J. Wang, R. Wolf, J. Caldwell, P. J. Kollman and D. J. Case, *J Comput Chem*, 2004, 25, 1157-1174.
48. B. Hess, *J Chem Theory Comput*, 2008, 4, 116-122.
49. D. Van Der Spoel, E. Lindahl, B. Hess, G. Greonhof, A. E. Mark and H. J. Berendsen, *J Comput Chem*, 2005, 26, 1701-1718.
50. B. Hess, C. Kutzner, D. Van Der Spoel and E. Lindahl, *J Chem Theory Comput*, 2008, 4, 435-447.
51. G. A. Tribello, M. Bonomi, D. Branduardi, C. Camilloni and G. Bussi, *Comput Phys Commun*, 2014, 185, 604-613.
52. F. Rossi, F. Castiglione, M. Ferro, P. Marchini, E. Mauri, M. Moioli, A. Mele and M. Masi, *Chemphyschem*, 2015, 16, 2818-2825.
53. F. Rossi, G. Perale, G. Storti and M. Masi, *J. Appl. Polym. Sci.*, 2012, 123, 2211-2221.
54. M. Santoro, P. Marchetti, F. Rossi, G. Perale, F. Castiglione, A. Mele and M. Masi, *J. Phys. Chem. B*, 2011, 115, 2503-2510.
55. P. J. Flory, *Principles of polymer chemistry*, Cornell Univeristy Press, New York, 1953.
56. S. J. de Jong, B. van Eerdenbrugh, C. F. van Nostrum, J. J. Kettenes-van de Bosch and W. E. Hennink, *J. Control. Release*, 2001, 71, 261-275.
57. J. Pang, Y. Luan, F. Li, X. Cai, J. Du and X. Li, *Int. J. Nanomed.*, 2011, 6, 659-665.
58. F. Castiglione, E. Ragg, A. Mele, G. B. Appetecchi, M. Montanino and S. Passerini, *J. Phys. Chem. Lett.*, 2011, 2, 153-157.
59. M. Ferro, F. Castiglione, C. Punta, L. Melone, W. Panzeri, B. Rossi, F. Trotta and A. Mele, *Beilstein J. Org. Chem.*, 2014, 10, 2715-2723.
60. K. Adrjanowicz, Z. Wojnarowska, M. Paluch and J. Pionteck, *J. Phys. Chem. B*, 2011, 115, 4559-4567.
61. A. R. Bras, J. P. Noronha, A. M. M. Antunes, M. M. Cardoso, A. Schonhals, F. Affouard, M. Dionisio and N. T. Correia, *J. Phys. Chem. B*, 2008, 112, 11087-11099.
62. P. L. Ritger and N. A. Peppas, *J. Control. Release*, 1987, 5, 23-36.
63. N. H. N. Kamarudin, A. A. Jalil, S. Triwahyono, M. R. Sazegar, S. Hamdan, S. Baba and A. Ahmad, *Rsc Adv*, 2015, 5, 30023-30031.
64. E. B. Schirmer and G. Carta, *AIche J.*, 2007, 53.
65. G. L. Frey and E. Grushka, *Anal Chem*, 1996, 68, 2147-2154.
66. R. B. Bird, W. E. Steward and E. N. Lightfoot, *Transport Phenomena*, Wiley-VCH, 2007.

View Article Online
DOI: 10.1039/C7CP00832E

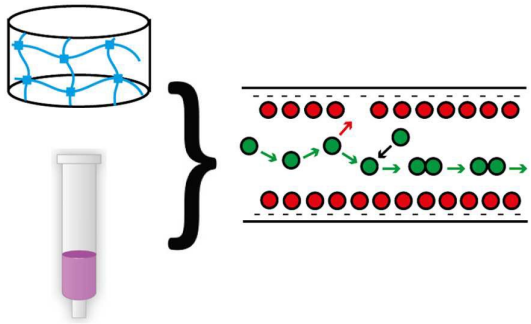

Solute motion in drug delivery and chromatography were compared to build a simple model able to rationalize the phenomena involved.